Ab Initio Quantum Chemical Investigation of the Ground and Excited States of Salicylic Acid Dimer

Shruti Maheshwary, U. Lourderaj, and N. Sathyamurthy*

Department of Chemistry, Indian Institute of Technology Kanpur, Kanpur 208 016 India

Received: June 7, 2006; In Final Form: September 21, 2006

The structure and stability of different forms of salicylic acid dimer have been examined by Hartree−Fock and density functional theoretic calculations using 6-31G(d,p) and 6-311++g(d,p) basis sets. Vertical excitation energies for the monomer as well as the dimer have been computed using the time-dependent density functional theory using 6-311++G(d,p) basis set. The predicted absorption maxima for the first excited singlet state of salicylic acid monomer and the dimer of the primary form are in reasonable agreement with the experimental result. There is a slight red shift (∼6 nm) in the absorption maximum in going from the monomer to the dimer, in accord with the experimental observation. Configuration-interaction calculations including single excitation have been carried out to map the potential-energy profile for the intra- as well as the intermolecular proton transfer in different forms of the dimer. The barrier for proton transfer in the ground state as well as the excited states makes it clear that most of the processes take place in the primary form and largely by intramolecular proton transfer.

1. Introduction

Salicylic acid (SA) and its derivatives have been the focus of attention of many experimental and theoretical studies over the years. Weller[1] had pointed out the dual emission in the fluorescence spectrum of salicylic acid and methyl salicylate and had attributed it to asymmetric double well potentials arising from proton transfer in the ground state and also in the excited state. Subsequently, several experimental[2−16] and theoretical[17−23] studies have been devoted to excited-state intramolecular proton transfer (ESIPT) processes in salicylic acid and related systems.

SA exists as a monomer in polar solvents,[11] and it gets protonated and deprotonated depending upon the pH of the solution.[10] Like most other carboxylic acids, it exists as a cyclic hydrogen-bonded dimer in solid state, in nonpolar solvents, and in gas phase at moderate and high concentrations.[8−10,12] As a monomer, it exists largely in primary (P) form and to some extent in rotamer (R) and tautomer (T) forms (see Figure 1). Therefore, it could, in principle, dimerize in six different ways: primary−primary (PP), rotamer−rotamer (RR), tautomer−tautomer (TT), primary−rotamer (PR), primary−tautomer (PT), and rotamer−tautomer (RT) (see Figure 2). SA dimer is perhaps the smallest aromatic system in which both intra- and intermolecular hydrogen bonding exists and thus constitutes an ideal model to study both modes of proton transfer in a single system.

Considerable effort has gone into the study of double-proton-transfer reactions (DPTRs), especially in cyclic dimers of carboxylic acid.[24−28] Formic acid dimer is, perhaps, the simplest such system that has been studied extensively, experimentally as well as theoretically, as it forms strong hydrogen bonds and it can be used as a model for many chemically and biologically important multi-proton-transfer systems. For recent work, the reader is referred to refs 27 and 28 and references therein. Most of the earlier studies had focused on the geometrical changes on dimerization and the energy stabilization due to hydrogen bond formation in the dimer.[29−31] Ernst and collaborators[32] studied the double proton transfer in crystalline benzoic acid dimer and measured the kinetic isotope effect and suggested predominant tunneling even at room temperature. 7-Azaindole and 1-azacarbazole dimers[33−35] are some of the well-studied systems that show large Stokes shifted emission from the corresponding tautomers resulting from excited-state DPTR. Recently, Chou et al.[36] have studied the analogues of 7-azaindole in which intact dual hydrogen-bonded dimers are formed in crystalline state and could mimic intrinsic excited-state double-proton-transfer dynamics.

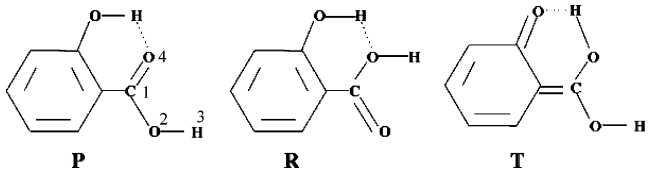

Figure 1. P, R, and T forms of salicylic acid.

Bisht et al.[12] studied the fluorescence and excitation spectra of SA dimer under supersonic nozzle beam expansion conditions and found them to be complicated because of the presence of two acidic protons, one on the carboxylic group and the other on the phenolic, which are partially exchanged. In condensed phase, SA seems to exist predominantly as a dimer, consisting of two units of R. Since dimerization of the P form involves weakening of the two intramolecular hydrogen bonds while forming intermolecular hydrogen bonds, the PP dimer becomes less stable when compared to the RR. Infrared and Raman spectroscopic studies of crystalline SA suggested an energy difference of 0.44 kcal/mol between the PP and RR forms.[7,8,37] The fluorescence excitation spectra[12] show a broad background, indicating the possibility of intermolecular double proton transfer. The emission spectrum consists of two broad bands of equal intensity with the maxima at ∼360 and ∼400 nm suggesting that the structure of the dimer in the first excited

* Author to whom correspondence should be addressed. E-mail: nsath@iitk.ac.in.

10.1021/jp063523n CCC: $33.50
Published on Web 11/02/2006

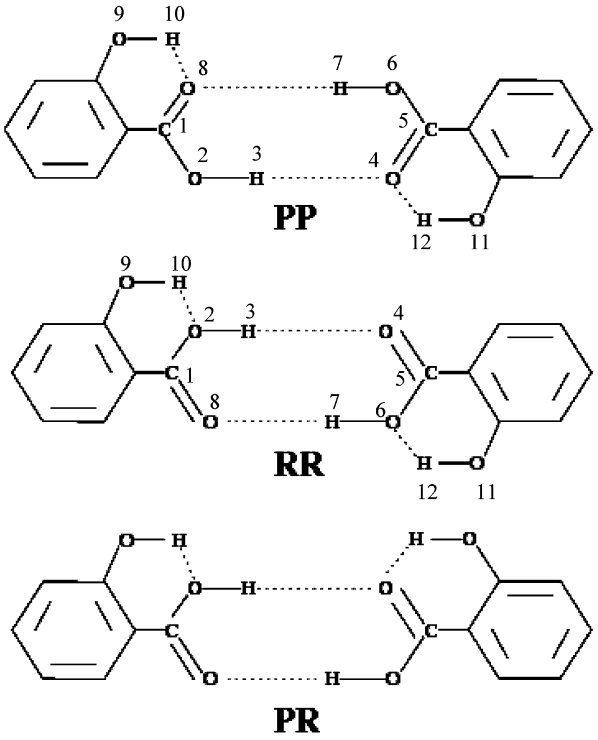

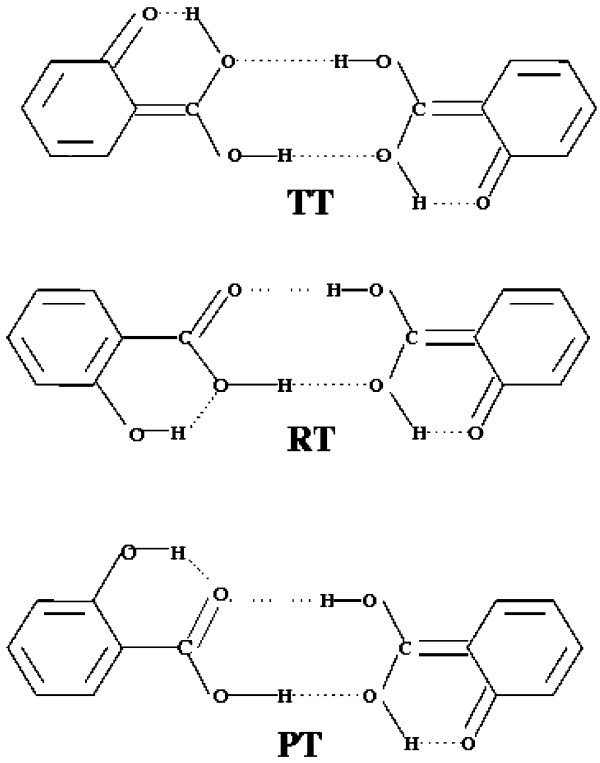

Figure 2. Six possible forms of dimers of salicylic acid.

singlet (S_1) state is intermediate between that of PP and RR or that there is rapid equilibration between the two. The dual emission of SA is found to be temperature and excitation wavelength dependent.[8,9]

To the best of our knowledge, there has been no ab initio quantum chemical calculation reported till this date on the structure and spectral properties of SA dimers or on the features of its potential energy curve for the inter- and intramolecular proton transfer in their ground and excited states. The relative stability and the barrier for interconversion of different structures have also not been reported. Therefore, an ab initio electronic structure investigation of SA dimer has been undertaken. While the methodology is briefly outlined in section 2, the results are presented and discussed in section 3. Summary and conclusions follow in section 4.

2. Methodology

Ground-state properties of the monomer and dimer of salicylic acid have been investigated using Hartree−Fock (HF) and density functional theoretic (DFT) methods using the 6-31G-(d,p) and 6-31++G(d,p) basis sets. Our earlier studies[22] had shown HF/6-31G(d,p) to be the optimal basis set in terms of price-performance ratio for carrying out elaborate potential-energy curve calculations for systems such as salicylic acid. Frequency calculations were carried out to ensure that the geometries obtained corresponded to minima and not saddle points. The excited states have been studied using configuration interaction including single excitation (CIS) method and time-dependent density functional theoretic (TDDFT) method using LDA and B3LYP functionals for the monomer as well as for the dimer. Calculations employing complete-active-space-self-consistent-field (CASSCF) and multireference configuration interaction (MRCI) methodologies could be carried out only for the monomer. The TDDFT, CASSCF, and MRCI calculations were performed using 6-311++G(d,p) basis set. All the HF and DFT calculations reported in this paper were carried out using the GAUSSIAN 94 or GAUSSIAN 98 suite of programs.[38,39] For CASSCF and MRCI calculations, the MOLPRO 2000.1 package[40] was used.

TABLE 1: Ground-State Geometric Parameters for Salicylic Acid Monomer

method	r_{12}/Å C−O	r_{23}/Å O−H	r_{14}/Å C=O	θ_{214}/deg O−C=O	θ_{123}/deg C−O−H
HF/6-311++G(d,p)[a]	1.322	0.946	1.197	121.0	108.4
DFT(B3LYP)/6-311++G(d,p)[a]	1.349	0.969	1.226	120.7	106.9
expt[b]	1.307		1.234	121.1	

[a] Present work. [b] Reference 42.

The dimerization energy for SA was calculated from the difference in energies between the dimer and the two monomers and was corrected for basis set superposition error (BSSE) using the counterpoise (CP) correction scheme proposed by Boys and Bernadi:[41]

$$E_{\text{dimer}}^{\text{CP}} = E_{\text{dimer}} + \text{CP} \tag{1a}$$

$$\text{CP} = \sum (E_{\text{mf}}^{\text{i}} - E_{\text{mf}}^{\text{i}}*) \tag{1b}$$

where E_{dimer} represents the (total) energy computed for the dimer, E_{mf}^{i} represents the energy of the individual monomer in its (frozen) geometry in the dimer, and the asterisk (*) represents the monomer energy calculated with "ghost" orbitals.

3. Results and Discussion

3.1. Geometries and Energetics of the Monomer. Optimized geometries and absorption maxima for the P and R forms obtained from HF/6-31G(d,p) and AM1 (PECI = 8) calculations were already reported in ref 22. More recent calculations at the HF/6-311++G(d,p) and DFT (B3LYP)/6-311++G(d,p) levels yield geometrical parameters for the ground state of the monomer (P form) in agreement with the X-ray crystal structure values[42] as shown in Table 1. The r_{12} (C−O) bond distance is

TABLE 2: Wavelengths in nm Units Corresponding to Vertical Excitation Energies for Salicylic Acid Monomer (P and R Forms), Obtained Using 6-311++G(d,p) Basis Set. Values in Parentheses Are the Excitation Energies in eV

		P form				R form		
excited state	major transition	TDDFT(LDA)	TDDFT(B3LYP)	CASSCF	MRCI	TDDFT(B3LYP)	expt [a]	oscillator strength[b]
S_1	6a″−7a″	332.7 (3.73)	297.0 (4.17)	203.4 (6.10)	216.9 (5.72)	290.2 (4.26)	311	0.0830
S_2	30a′−7a″	286.6 (4.33)	242.4 (5.11)	170.2 (7.29)	189.6 (6.91)	241.8 (5.13)		0.0
S_3	5a″−7a″	273.9 (4.53)	235.2 (5.27)	161.4 (7.69)		234.6 (5.29)		0.1336
T_1	6a″−7a″	412.2 (3.01)	381.8 (3.25)	262.9 (4.72)	266.3 (4.66)	371.2 (3.34)		
T_2	5a″−7a″	332.1 (3.73)	347.6 (3.57)	253.8 (4.89)	260.1 (4.77)	347.8 (3.56)		
T_3	6a″−8a″	318.2 (3.90)	289.9 (4.28)	217.7 (5.70)	228.9 (5.42)	288.7 (4.29)		

[a] In cyclohexane from ref 8. [b] For the P form at DFT(B3LYP)/6-311++G(d,p) level of theory.

TABLE 3: Relative Energies, Strength of Intramolecular Hydrogen Bonds (I_{ntra}MHBs), and Dimerization Energy for Different Forms of Salicylic Acid Dimer in Their Ground Electronic States in kcal/mol Units[a]

	HF	DFT(B3LYP)	
	6-31G(d,p)	6-31G(d,p)	6-311++G(d,p)
	Relative Stability		
PP	0.0	0.0	0.0
PR	2.4	2.6	
RR	4.7	4.9	4.2, 3.9[b]
PT	25.4	25.3	
RT	29.3		
TT	52.2	50.9	
	Strength of I_{ntra}MHBs		
PP (C═O···H−O + C═O···H−O)	20.8		
RR (C−O···H−O + C−O···H−O)	15.5		
PR (C−O···H−O + C═O···H−O)	18.1		
PT (C═O···H−O + C═O···H−O)	15.3		
RT (C−O···H−O + C═O···H−O)	19.5		
TT (C═O···H−O + C═O···H−O)	18.7		
	Dimerization Energy		
PP	−14.7 (−12.7)	−14.4	−15.5 (−14.5),−14.7[b]
PR	−15.9 (−13.8)	−15.3	
RR	−17.3 (−15.1)	−16.5	−18.2 (−17.3),−17.2[b]
PT	−12.8 (−11.1)	−11.3	
RT	−12.5		
TT	−9.5 (−8.3)	−7.9	

[a] The values in parentheses are corrected for basis set superposition error. [b] Zero-point energy corrected values.

overestimated by both HF and DFT calculations by 0.015 and 0.042 Å, respectively. The DFT predicted C═O bond length is only 0.008 Å less than the experimental value, while the HF calculations underestimate it further (0.037 Å). The optimized geometries for the ground state were used for the excited-state calculations. For the CASSCF calculations, eight active orbitals comprised of n, π, π^*, and σ^* orbitals (with six electrons) as the active space were used. For the MRCI calculation, seven orbitals (with six electrons) were used as the active space. The vertical excitation energies calculated from TDDFT (LDA, B3LYP), CASSCF, and MRCI methods for the P form of the monomer are reported in the form of absorption maxima in Table 2.

The transition involved for the first singlet and triplet excited states is of $\pi-\pi^*$ (6a″−7a″) type, while the second excited singlet state is due to $n-\pi^*$ (30a′−7a″) transition. TDDFT (B3LYP) calculations predict an absorption wavelength of 297.0 nm, close to the experimental result of 311 nm.[8] The former is comparable to the value of 295.5 nm, reported from TDDFT-(B3LYP)/cc-pvDZ calculations by Sobolewski and Domcke,[43] and 316.5 nm, reported by the same authors using CASPT2 method.[21] TDDFT (LDA) calculation predicts a slightly larger excitation wavelength. Both CASSCF and MRCI calculations predict a much larger excitation energy and hence smaller wavelength presumably because of the small active space used. The improvement in the accuracy of the calculations with increase in active space can be seen from the CASPT2 results reported by Sobolewski and Domcke.[43]

3.2. Geometries and Energetics of the Dimer. The six different dimers of SA can be classified into homo and hetero types, depending upon whether the same or different monomeric species interact to form the dimer. The dimers PP, RR, and TT belong clearly to the homo variety while the others (PR, PT, and RT) belong to the hetero variety. All homo dimers are of C_{2h} symmetry, while the hetero dimers belong to C_s symmetry.

Hartree−Fock calculations were carried out using 6-31G(d,p) basis set for the different possible dimers, and their geometries were optimized without imposing any constraint, unless one of the monomeric units was T. Some of the salient aspects of the relative stability, the strength of intramolecular hydrogen bonds, and the dimerization energy for the different dimers are presented in Table 3. The most stable form is the PP dimer, with two equivalent O−H···O═C intermolecular hydrogen bonds (I_{nter}MHBs) and two C═O···H−O− type intramolecular hydrogen bonds (I_{ntra}MHBs). The strength of the two I_{ntra}MHBs was found to be 20.8 kcal/mol (or 10.4 kcal/mol per I_{ntra}MHB), when compared to 11.0 kcal/mol reported for the monomer P.[22] The strength of the I_{ntra}MHB was calculated by rotating the intramolecular hydrogen-bonded phenolic −OH out by 180° and reoptimizing the rest of the geometry. Clearly, there is a slight weakening of the intramolecular hydrogen bonds because of the formation of intermolecular hydrogen bonds. The BSSE uncorrected dimerization energy for the PP dimer is −14.7 kcal/mol and with BSSE correction it comes to −12.7 kcal/mol (see Table 3). DFT(B3LYP) calculations using a significantly larger

TABLE 4: Comparison of the Ground-State Optimized Geometric Parameters for the Monomer (P, R) and the Dimers (PP, RR) of Salicylic Acid with the Monomer and Dimer of Benzoic Acid as Obtained from DFT(B3LYP)/6-311++G(d,p) Calculation[a]

	SA		SA		BA[b]	
parameter	monomer (P)	dimer (PP)	monomer (R)	dimer (RR)	monomer	dimer
C−O/Å	1.349	1.318 (1.307)	1.379	1.338	1.359	1.322
O−H/Å	0.969	0.997 (1.002)	0.969	1.006	0.968	0.999
O···H/Å(inter)		1.676 (1.653)		1.618		1.660
O···H/Å(intra)	1.764	1.758 (1.704)	1.803	1.794		
C═O/Å	1.226	1.247 (1.234)	1.205	1.230	1.209	1.230
O···O/Å		2.674 (2.653)		2.625		2.664
O−H···O/deg		179.3 (178.4)		179.8		175.3
H···O═C/deg		127.0 (126.8)		127.3		126.8
υ_{O-H}/cm^{-1}	3619	3105	3619	2956	3621	3073
		3025		2853		2984
$\upsilon_{C=O}/cm^{-1}$	1659	1623	1723	1658	1714	1662
		1566		1617		1618

[a] The vibrational frequencies are scaled by a factor of 0.96. The experimental geometrical parameters[42] are given in parentheses. [b] From ref 28.

basis set 6-311++G(d,p) yielded a dimerization energy of −14.5 kcal/mol (after BSSE correction).

The RR dimer is higher in energy than the PP by 4.7 kcal/mol. It has two equivalent C−O···H−O I_{ntra}MHBs present. The strength of both the I_{ntra}MHBs is calculated to be 15.5 or 7.75 kcal/mol per I_{ntra}MHB.

The PR dimer is less stable than the PP by 2.4 kcal/mol because of the presence of the R unit, which is known to be higher in energy than the P. The strength of the I_{ntra}MHB corresponding to the R monomeric unit in the PR dimer is 7.3 kcal/mol, when compared to 6.6 kcal/mol for the isolated R. This was computed by breaking the I_{ntra}MHB present in R by rotating the phenolic −OH out by 180°, while retaining the I_{ntra}MHB in P. The strength of the I_{ntra}MHB in P in the PP dimer was already shown to be 10.4 kcal/mol (see above). The strength of both the I_{ntra}MHBs in PR, when added, comes out to be (10.4 + 7.75 =) 18.15 kcal/mol, when compared to the directly computed value of 18.1 kcal/mol.

The PT, RT, and TT dimers are understandably much higher in energy than the other three dimeric forms, because of the presence of the T monomeric unit, which is known to be unstable because of the partial loss of aromaticity of the benzene ring.[19] The PT form is higher in energy by 25.4 kcal/mol, when compared to the PP.

The RT dimer is formed by the interaction of R and T monomers and has O−H···O═C and O−H···O−C═ type of I_{nter}MHBs, and C−O···H−O and C═O···H−O═ I_{ntra}MHBs. The RT dimer is less stable than the PP by 29.3 kcal/mol. The TT dimer is the least stable of all six dimers investigated.

Values of bond distances and bond angles involved in the dimer, as obtained from geometry optimization at DFT(B3LYP)/6-311G++(d,p) level for PP and RR dimers, are compared in Table 4. The reported geometrical parameters for the PP dimer are in good agreement with the experimental results.[42] The C−O bond distances decrease during the dimerization, and the O−H and the C═O bond distances increase. That the changes in the bond distances during dimerization are due to hydrogen bond formation is confirmed by natural bond orbital (NBO) analysis. Table 5 lists the changes in electron density in the lone pairs (n) and the antibonding (σ^*, π^*) NBOs during the formation of dimer in PP and RR forms. The lone pair (O8) and the antibonding orbital (σ^*) of C1−O2 show a large decrease in electron density that results in strengthening of the C−O bond and hence the observed decrease in the bond distance. There is also an increase in the electron density of the antibonding orbital σ^* of O−H and π^* of C═O in the RR dimer. This weakens the O−H and C═O bonds resulting in lengthening of the bond distances. In PP dimer, a similar increase in the electron density of the antibonding orbital σ^* of O−H and lengthening of the O−H bond is observed. However, the π^* antibonding orbital changes its nature and is more localized as a nonbonding orbital of O8. This is presumably because of the formation of the intramolecular hydrogen bond. The interaction between the filled donor NBO (i) and the vacant acceptor NBO (j) can be approximated by second-order perturbation theoretic expression

$$E(2) = -n_i \frac{\langle i|F|j\rangle^2}{\epsilon_j - \epsilon_i} = -n_i \frac{F_{ij}^2}{\Delta E} \qquad (2)$$

where ϵ_i and ϵ_j are NBO energies, n_i is the occupancy of the donor orbital, and F_{ij} is the Fock matrix element. These second-order perturbative interaction energies between the NBOs are listed in Table 6. There exists a large interaction between the lone pair (n) of the carbonyl oxygen and the antibonding (σ^*)

TABLE 5: Changes in the Electron Density in the Lone Pair (n) and Antibonding (σ^*, π^*) Orbitals on Dimerization for the PP and RR Forms of Salicylic Acid Dimer[a]

NBO	PP	RR
n (O8)	−0.02624	−0.02567
n (O8)	+0.00988	+0.00572
σ^* (C1−O8)	+0.00603	+0.00581
π^* (C1−O8)		+0.06333
σ^* (C1−O2)	−0.02241	−0.03338
σ^* (O2−H3)	+0.05393	+0.0677
σ^* (O9−H10)	−0.00216	+0.00305

[a] The atom labels are defined in Figure 2. Because of symmetry, results are shown only for one of the monomer units in the dimer.

TABLE 6: Second-Order Perturbation Theoretic Analysis of the Interaction between Electron Donor and Acceptor Orbitals in NBO Basis[a]

donor NBO (i)	acceptor NBO (j)	$E(2)$[b] (kcal/mol)	$\epsilon_j - \epsilon_i$[c] (a.u.)	F_{ij}[d] (a.u.)
Salicylic Acid Dimer[e] (PP)				
LP(1)O8	BO*(1)O6−H7	11.07	1.12	0.100
LP(2)O8	BO*(1)O6−H7	15.33	0.70	0.094
Salicylic Acid Dimer[e] (RR)				
LP(1)O8	BO*(1)O6−H7	10.30	1.06	0.094
LP(2)O8	BO*(1)O6−H7	25.48	0.70	0.122

[a] See Figure 2 for atom labels. Because of symmetry, unit 2 to unit 1 results are not shown. [b] Hyperconjugative interaction energy. LP and BO represent lone pair and bonding orbitals. [c] Energy difference between donor (i) and acceptor (j) NBOs. [d] Fock matrix element between (i) and (j) NBOs. [e] From unit 1 to unit 2.

TABLE 7: Wavelengths (in nm Units) Corresponding to Vertical Excitation Energies of PP and RR Forms of Salicylic Acid Dimer Using 6-311++G(d,p) Basis Set. Values in Parentheses Are the Excitation Energies in eV

		PP			RR		
excited state	major transition	TDDFT (LDA)	TDDFT (B3LYP)	oscillator strength	TDDFT (LDA)	TDDFT (B3LYP)	expt[a]
S_1	$6b_g-7a_u$	400.3 (3.09)	304.2 (4.08)	0.191	311.0 (3.99)	300.4 (4.13)	315 (3.94)
S_2	$6a_u-7a_u$	399.5 (3.10)	302.1 (4.10)	0.0	308.0 (4.03)	298.7 (4.15)	
S_3	$6b_g-7b_g$	337.1 (3.68)	287.9 (4.31)	0.0	293.5 (4.22)	286.6 (4.33)	
S_4	$6a_u-7b_g$	335.5 (3.70)	287.3 (4.32)	0.0123	293.1 (4.23)	286.5 (4.33)	
T_1	$6b_g-7a_u$	426.0 (2.91)	386.8 (3.21)		396.1 (3.13)	380.5 (3.26)	
T_2	$6a_u-7a_u$	423.8 (2.93)	386.6 (3.21)		395.7 (3.13)	380.2 (3.26)	
T_3	$5b_g-7a_u$	392.7 (3.16)	348.7 (3.56)		344.4 (3.60)	349.7 (3.55)	
T_4	$5a_u-7a_u$	390.7 (3.17)	348.6 (3.56)		344.0 (3.60)	349.6 (3.55)	

[a] In cyclohexane, from ref 8.

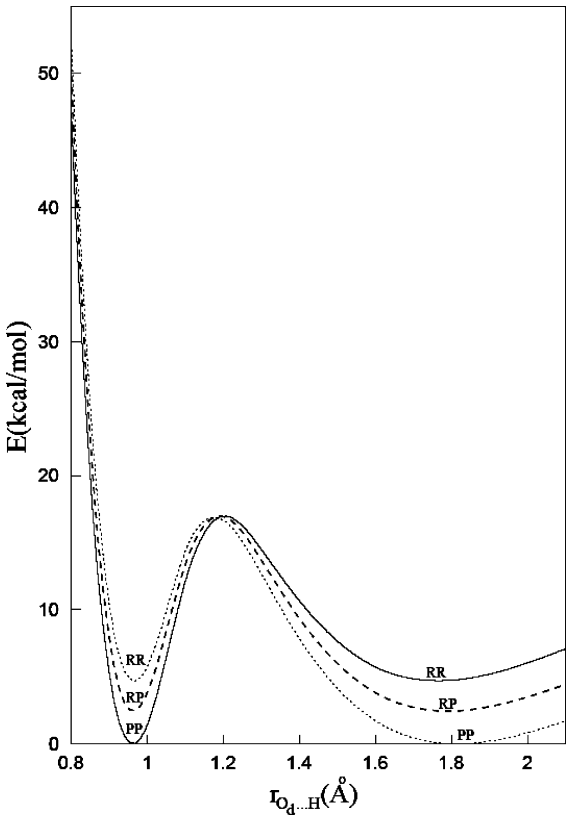

Figure 3. PE profiles for double proton transfer in the ground state for different forms of SA dimer, as obtained from HF/6-31G** calculation.

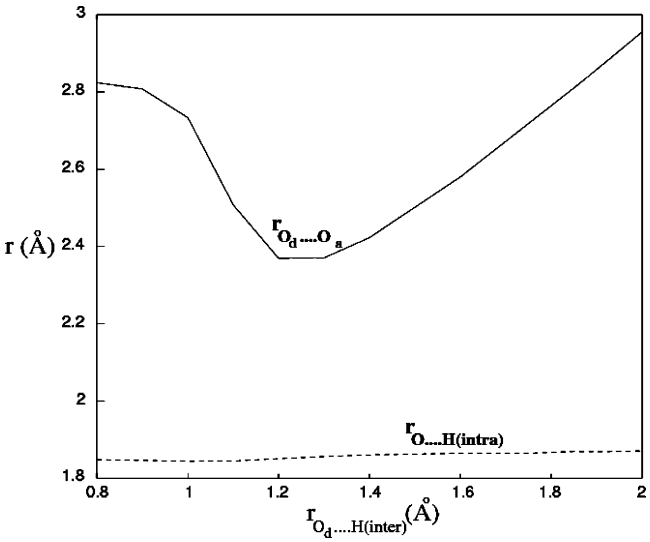

Figure 4. Variation of the $O_d\cdots O_a$ distance and intramolecular O···H distance with r_{Od-H}, in intermolecular double proton transfer as obtained from HF/6-31G** basis set calculations for SA dimer (PP).

NBO of O−H, implying a stronger interaction between the monomer units, that is, stronger hydrogen bond. The interactions are larger for the RR dimer than for the PP dimer resulting in shorter O···H bonds, longer O−H bonds, and larger dimerization energy for the RR dimer than for the PP. The changes in electron density and the resulting stronger hydrogen bonds are also reflected in the observed red shifts in the stretching frequencies of C═O and O−H. Because of the reasons discussed above, the RR dimer shows larger red shifts than the PP dimer upon dimerization (see Table 4).

It is interesting to see the effect of O−H in the β-position to the carbonyl group on the dimerization of salicylic acid by comparing the PP and RR dimers with benzoic acid dimer (BAD)[28] (Table 4). The presence of O−H on the side of the C═O group in P has a slight destabilizing effect, while O−H on the side of C−O−H in R has a stabilizing effect. The binding energies follow the order PP $\approx$ BAD < RR. The C═O bond length decreases in the order PP > BAD $\approx$ RR, while the C−O bond length increases as PP $\approx$ BAD < RR. The intermolecular hydrogen bond distances (O···H, O···O) increase as RR < PP $\approx$ BAD. It is clear that the dimerization energy and the ground-state geometrical properties of BAD are comparable to those of the PP form of SAD. The ground-state geometrical parameters for the PR dimer were estimated at HF/6-31G(d,p) level of theory. There is a decrease in the O···H (intra) distance in R, but the value of O···H (intra) distance in P remains unaltered (not reported).

The excited states of PP and RR forms have been investigated using the TDDFT (LDA and B3LYP) method and 6-311++G-(d,p) basis set. The resulting vertical excitation energies are listed in Table 7. All the excited singlet and the triplet states reported result from $\pi-\pi^*$ transitions involving excitations from $6b_g$, $6a_u$, $5b_g$, and $5a_u$ orbitals to $7a_u$ and $7b_g$. Both the PP and RR forms exhibit similar transitions as well as transition energies. The excited states appear nearly as doublets as they arise from the symmetric double-well potential for proton transfer in the homo dimer. A similar behavior has been observed for benzoic acid dimer, for example.[28] TDDFT(B3LYP) results for the absorption maxima for the PP form differ from those for RR only by a few nm. The predicted absorption wavelength values for the S_0-S_1 transition for PP and RR are comparable to the experimental results. The predicted red shift in the excitation wavelength value in going from the monomer to the dimer of salicylic acid (λ (P) = 297.6 nm, λ (PP) = 304.2 nm) is in qualitative agreement with the experimental result[8] (λ_{max} (monomer) = 311 nm, λ_{max} (dimer) = 315 nm).

3.3. Inter- and Intramolecular Proton Transfer in SA Dimer. To understand the photophysics of SA dimer, one has to go beyond simple λ_{max} calculations. Potential energy curves

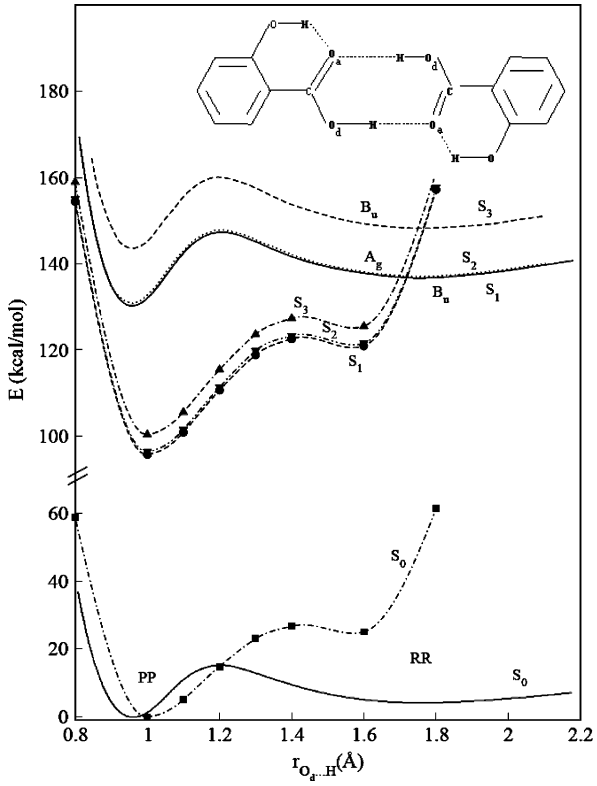

Figure 5. Potential energy profile for intermolecular double proton transfer in the ground state (S_0) of PP dimer as obtained from HF/6-31G** calculations and for some of the excited states as obtained from a CIS calculation. The dashed lines with data point symbols represent DFT calculations for the ground state and TDDFT calculations for the excited states using B3LYP parametrization and 6-31G** basis set.

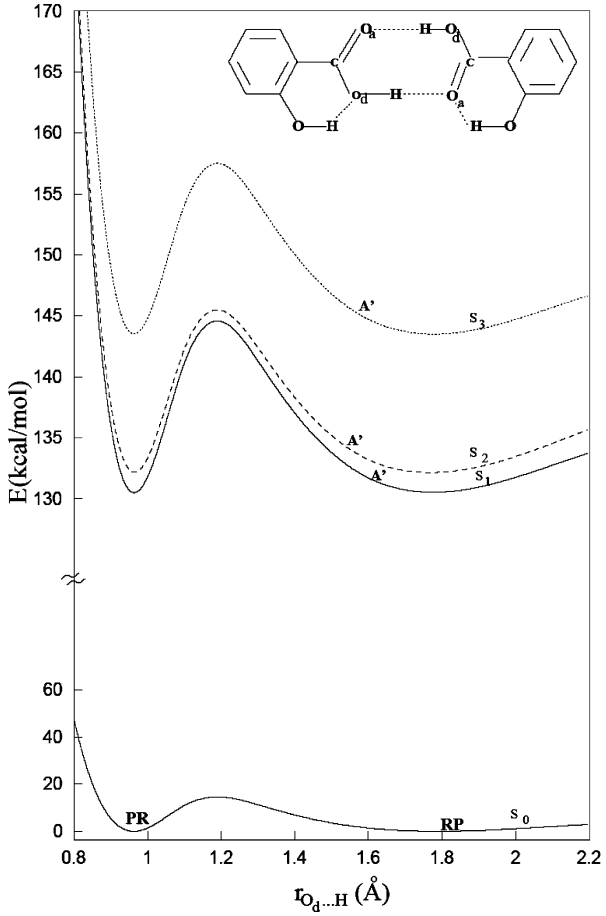

Figure 6. Potential energy profile for intermolecular double proton transfer in the ground state (S_0) of PR dimer as obtained from HF/6-31G** calculations and for some of the excited states as obtained from a CIS calculation.

for intermolecular proton transfer (I_{nter}PT) and intramolecular proton transfer (I_{ntra}PT) in the ground and excited states were generated for different dimers using HF/6-31G(d,p) and CIS/6-31G(d,p) calculations. The reaction coordinate was taken to correspond to the simultaneous motion of H atoms of one carboxylic acid group toward the carbonyl O atom of the other in the case of intermolecular proton transfer and the $O_d\cdots H$ distance within the monomer in the case of intramolecular proton transfer. For each value of the reaction coordinate, all other geometric variables were optimized for the ground state, and the vertical excitation energies were computed. Here, O_d refers to the donor oxygen atom.

PE curves for double proton transfer in the ground state of PP, PR, and RR dimers reveal two minima as shown in Figure 3. In the case of the PP dimer, the minimum at larger $r_{Od}\cdots H$ corresponds to the RR dimer, that is higher in energy by 2.6 kcal/mol. The barrier to proton transfer is calculated to be 16.9 kcal/mol.

Analysis of the changes in the structure of the dimer as the proton-transfer progresses shows that the $O_d\cdots O_a$ distance decreases initially and then it increases as illustrated in Figure 4. A similar behavior was found for the monomer also.[22] Here, O_a refers to the acceptor oxygen atom.

PE curves for proton transfer in the first three excited singlet states for the PP dimer are shown, along with the PE curve for the ground-state intermolecular proton transfer (GSI_{nter}PT) in Figure 5. In the excited states also the PP dimer is more stable than the RR. The barrier height to proton transfer in S_1 and S_2 is 15.5 kcal/mol. It is clear from the PE curves that there would be no Stokes shifted emission arising from excited-state intermolecular proton transfer (ESI_{nter}PT) in SA dimer. To see the effect of correlation, DFT calculations for the ground state and TDDFT calculations for the excited states were carried out using B3LYP parametrization and 6-31G(d,p) basis set. The potential energy profiles were mapped by studying the simultaneous motion of H atoms of one carboxylic group toward the carbonyl O atom of the other, using the ground-state equilibrium geometry of PP dimer. The results plotted in Figure 5 show that the barriers predicted by the density functional theoretic calculations are larger and that they occur farther along the proton-transfer coordinate, when compared to those obtained from CIS calculations. However, there is no noticeable shift in the emission wavelength because of ESI_{nter}PT in PP form. As was obtained from CIS calculations, the barrier heights (~27 kcal/mol) are nearly identical for the S_1 and S_2 states. Intermolecular proton transfer in PR dimer results in an equivalent conformation. The barrier height for the process is 14.5 kcal/mol, in the ground state as well as the first excited state (see Figure 6).

In PP dimer, one could also view intramolecular proton transfer in the presence of intermolecular hydrogen bonds resulting in PT or TT dimer, depending upon whether single or double intramolecular proton transfer takes place. During intramolecular double proton transfer, intermolecular distances remain constant and intramolecular $O_d\cdots O_a$ distances follow the same trend as observed for the monomer.

PE profiles for a single intramolecular proton transfer as obtained from a CIS calculation are reproduced in Figure 7 for the ground and the first excited singlet state. Such a transfer results in the PT dimer. It is clear from the figure for the ground

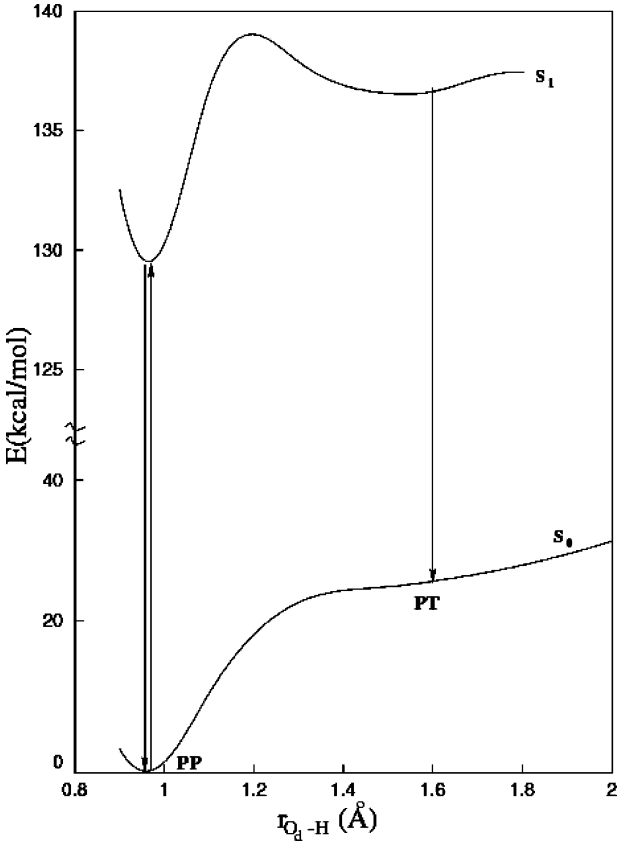

Figure 7. Potential energy profile for intramolecular single proton transfer in the ground state (S_0) of PP dimer as obtained from HF/6-31G** calculations and for the first excited singlet state as obtained from a CIS calculation.

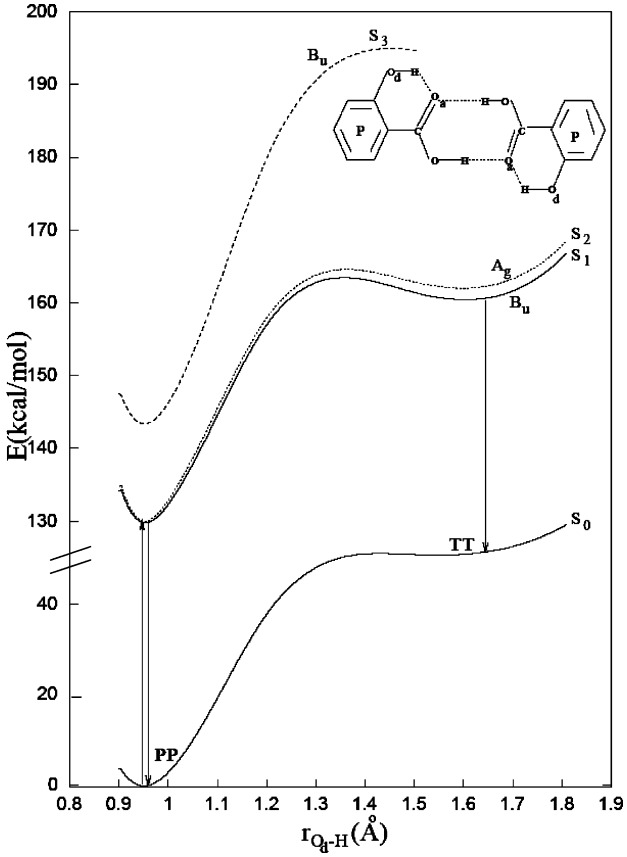

Figure 8. Potential energy profile for intramolecular double proton transfer in the ground state (S_0) of PP dimer as obtained from HF/6-31G** calculations and for some of the excited states as obtained from a CIS calculation.

state that there is one deep minimum corresponding to the PP dimer and a shallow minimum for the PT dimer. The barrier height to proton transfer is 25 kcal/mol. For the first excited singlet state, two minima are observed and the deeper minimum still corresponds to the PP dimer. There is a significant decrease in the barrier height (7.0 kcal/mol) to proton transfer. This suggests that if the excitation energy exceeds the barrier height a large Stokes-shifted emission would be observed.[9]

PE profiles for a double intramolecular proton transfer in the ground and excited states of PP dimer are shown in Figure 8. The transfer results in TT, the transition between S_0 and S_1 states corresponds to $\pi-\pi^*$, and a Stokes-shifted emission is expected. There is a large barrier (51.2 kcal/mol) to proton transfer in the ground state. Although the barrier height is lower in the excited state, it is still high (30.4 kcal/mol), thus requiring a large excitation energy to enable ESIPT. This would explain the experimentally observed excitation wavelength dependence of dual emission in SA dimer.[9]

4. Summary and Conclusion

The relative stabilities, strength of hydrogen bonds, and dimerization energies of six possible dimer structures of salicylic acid have been investigated at HF and DFT levels of theory. The PP dimer is clearly the most stable, followed by PR, RR, PT, RT, and TT. The dimerization energy is greater for RR than for PP, suggesting a greater stabilization of RR because of strengthening of intramolecular hydrogen bonds accompanying intermolecular hydrogen bonds. All the dimers could be interconverted by inter- or intramolecular proton transfer. TDDFT(B3LYP)/6-311++G(d,p) calculations predict vertical excitation energies for the P form of the monomer and its dimer (PP) in very good agreement with the experimental values. That there is a nominal red shift in going from the monomer to the dimer is clearly accounted for by the TDDFT calculations.

PE profiles for proton transfer in salicylic acid dimer obtained using HF and CIS calculations suggest that single/double intramolecular and not intermolecular proton transfer is responsible for the experimentally observed dual emission. In the case of the single proton transfer, the excited-state barrier for S_1 is 7.0 kcal/mol, and in the case of the double proton transfer it is 30.4 kcal/mol. That the red-shifted emission observed experimentally is excitation wavelength dependent is explained by the substantial barrier to proton transfer in the excited state.

Acknowledgment. We are grateful to Dr. Hirdyesh Mishra for valuable discussions. We wish to thank Prof. Kihyung Song, Korea National University of Education, for extending computational resources. This study was supported in part by a grant from the Council of Scientific and Industrial Research, New Delhi. N.S. is grateful to the Department of Science and Technology, New Delhi for the award of J. C. Bose Fellowship.

References and Notes

(1) Weller, A. *Naturwissenchaften* **1955**, *42*, 175; *Z. Elektrochem.* **1956**, *60*, 1144; *Prog. React. Kinet.* **1961**, *1*, 187.

(2) Herek, J. L.; Pedersen, S.; Bañares, L.; Zewail, A. H. *J. Chem. Phys.* **1992**, *97*, 9046.

(3) Klopffer, W. *Adv. Photochem.* **1977**, *10*, 311.

(4) Woolfe, G. J.; Thistlethwaite, P. J. *J. Am. Chem. Soc.* **1980**, *102*, 6917; **1981**, *103*, 3849.

(5) Smith, K. K.; Kaufmann, K. J. *J. Phys. Chem.* **1981**, *85*, 2895.

(6) Torobio, F.; Catalán, J.; Amat, F.; Acuña, A. U. *J. Phys. Chem.* **1983**, *87*, 817.

(7) Joshi, H. C.; Tripathi, H. B.; Pant, T. C.; Pant, D. D. *Chem. Phys. Lett.* **1990**, *173*, 83.

(8) Pant, D. D.; Joshi, H. C.; Bisht, P. B.; Tripathi, H. B. *Chem Phys.* **1994**, *185*, 137.

(9) Bisht, P. B.; Tripathi, H. B.; Pant, D. D. *J. Photochem. Photobiol., A: Chem.* **1995**, *90*, 103.

(10) Joshi, H. C.; Mishra, H.; Tripathi, H. B. *J. Photochem. Photobiol., A: Chem.* **1997**, *105*, 15.

(11) Kovi, P. J.; Miller, C. L.; Schulman, S. G. *Anal. Chim. Acta* **1972**, *61*, 7.

(12) Bisht, P. B.; Petek, H.; Yoshihara, K.; Nagashima, U. *J. Chem. Phys.* **1995**, *103*, 5290.

(13) Bisht, P. B.; Okamoto, M.; Hirayama, S. *J. Phys. Chem. B* **1997**, *101*, 8850.

(14) Lahmani, F.; Zehnacker-Rentien, A. *J. Phys. Chem. A* **1997**, *101*, 6141.

(15) Humbert, B.; Alnot, M.; Quilés, F. *Spectrochim. Acta A* **1998**, *54*, 465.

(16) Denisov, G. S.; Golubev, N. S.; Schreiber, V. M.; Shajakhmedov, Sh. S.; Shurukhina, A. V. *J. Mol. Struct.* **1996**, *381*, 73; **1997**, *436*, 153.

(17) Catalán, J.; Fernandez-Alonso, J. I. *Chem. Phys. Lett.* **1973**, *18*, 37; *J. Mol. Struct.* **1975**, *27*, 59.

(18) Vener, M. V.; Scheiner, S. *J. Phys. Chem.* **1995**, *99*, 642.

(19) Sobolewski, A. L.; Domcke, W. *Chem. Phys*. **1994**, *184*, 115.

(20) Mitra, S.; Das, R.; Bhattacharyya, S. P.; Mukherjee, S. *J. Phys. Chem. A* **1997**, *101*, 293.

(21) Sobolewski, A. L.; Domcke, W. *Chem. Phys*. **1998**, *232*, 257.

(22) Maheshwari, S.; Chowdhury, A.; Sathyamurthy, N.; Mishra, H.; Tripathi, H. B.; Panda, M.; Chandrasekhar, J. *J. Phys. Chem. A* **1999**, *103*, 6257.

(23) Nagaoka, S.; Nagashima, U. *Chem. Phys.* **1989**, *136*, 153.

(24) Morita, H.; Nagakura, S. *J. Mol. Spectrosc.* **1972**, *42*, 536.

(25) Nagaoka, S.; Terao, T.; Imashiro, F.; Saika, A.; Hirota, N.; Hayashii, S. *Chem. Phys. Lett.* **1981**, *80*, 580; Nagaoka, S.; Terao, T.; Imashiro, F.; Saika, A.; Hirota, N. *J. Chem. Phys.* **1983**, *79*, 4694.

(26) Meier, B. H.; Graf, F.; Ernst, R. R. *J. Chem. Phys.* **1984**, *76*, 767.

(27) Gora, R. W.; Grabowski, S. J.; Leszczynski, J. *J. Phys. Chem. A* **2005**, *109*, 6397.

(28) Lourderaj, U.; Giri, K.; Sathyamurthy, N. *J. Phys. Chem. A* **2006**, *110*, 2709.

(29) Lazaar, K. I.; Bauer, S. H. *J. Am. Chem. Soc*. **1985**, *107*, 3679.

(30) Almenningen, A.; Bastiansen, O.; Motzfeldt, T. *Acta Chem. Scand.* **1970**, *24*, 747.

(31) Karpfen, A. *Chem. Phys*. **1984**, *88*, 415.

(32) Meyer, R.; Ernst, R. R. *J. Chem. Phys.* **1990**, *93*, 5518. Stöckli, A.; Meier, B. H.; Kreis, R.; Meyer, R.; Ernst, R. R. *J. Chem. Phys.* **1990**, *93*, 1502.

(33) Taylor, C. A.; El-Bayoumi, M. A.; Kasha, M. *Proc. Natl. Acad. Sci. (USA*) **1969**, *63*, 253.

(34) Chang, C.; Shabestary, N.; El-Bayoumi, M. A. *Chem. Phys. Lett.* **1980**, *75*, 107.

(35) Waluk, J.; Grabowska, A.; Pakula, B.; Sepiol, J. *J. Phys. Chem.* **1984**, *88*, 1160. Waluk, J.; Pakula, B. *J. Mol. Struct.* **1984**, 114, 359. Fuke, K.; Yabe, T.; Chiba, N.; Kohida, N.; Kaya, K. *J. Phys. Chem*. **1986**, *90*, 2309.

(36) Chou, P.-T.; Liao, J.-H.; Wei, C.-Y.; Yang, C.-Y.; Yu, W.-S.; Chou, Y.-H. *J. Am. Chem. Soc.* **2000**, *122*, 986.

(37) Upadhyay, P.; Pant, D. D.; Bist, H. D. In *Proceedings of the XII International Conference on Raman Spectroscopy*; Durig, J. R., Sullivan, J. P., Eds.; Wiley: Singapore, 1990.

(38) Frisch, M. J.; Trucks, G. W.; Schlegel, H. B.; Gill, P. M. W.; Johnson, B. G.; Robb, M. A.; Cheeseman, J. R.; Keith, T.; Petersson, G. A.; Montgomery, J. A., Jr.; Raghavachari, K.; Al-Laham, M. A.; Zakrzewski, V. G.; Ortiz, J. V.; Foresman, J. B.; Cioslowski, J.; Stefanov, B. B.; Nanayakkara, A.; Challacombe, M.; Peng, C. Y.; Ayala, P. Y.; Chen, W.; Wong, M. W.; Andres, J. L.; Replogle, E. S.; Gomperts, R.; Martin, R. L.; Fox, D. J.; Binkley, J. S.; Defrees, D. J.; Baker, J.; Stewart, J. J. P.; Head-Gordon, M.; Gonzalez, C.; Pople, J. A. *Gaussian 94*, Revision C.2; Gaussian Inc.: Pittsburgh, PA, 1995.

(39) Frisch, M. J.; Trucks, G. W.; Schlegel, H. B.; Scuseria, G. E.; Robb, M. A.; Cheeseman, J. R.; Zakrzewski, V. G.; Montgomery, J. A., Jr.; Stratmann, R. E.; Burant, J. C.; Dapprich, S.; Millam, J. M.; Daniels, A. D.; Kudin, K. N.; Strain, M. C.; Farkas, O.; Tomasi, J.; Barone, V.; Cossi, M.; Cammi, R.; Mennucci, B.; Pomelli, C.; Adamo, C.; Clifford, S.; Ochterski, J.; Petersson, G. A.; Ayala, P. Y.; Cui, Q.; Morokuma, K.; Salvador, P.; Dannenberg, J. J.; Malick, D. K.; Rabuck, A. D.; Raghavachari, K.; Foresman, J. B.; Cioslowski, J.; Ortiz, J. V.; Baboul, A. G.; Stefanov, B. B.; Liu, G.; Liashenko, A.; Piskorz, P.; Komaromi, I.; Gomperts, R.; Martin, R. L.; Fox, D. J.; Keith, T.; Al-Laham, M. A.; Peng, C. Y.; Nanayakkara, A.; Challacombe, M.; Gill, P. M. W.; Johnson, B.; Chen, W.; Wong, M. W.; Andres, J. L.; Gonzalez, C.; Head-Gordon, M.; Replogle, E. S.; Pople, J. A. *Gaussian 98*, Revision A.11.1; Gaussian, Inc.: Pittsburgh, PA, 2001.

(40) MOLPRO is a package of ab initio programs written by Werner, H.-J.; Knowles, P. J. with contributions from Amos, R. D.; Bernhardsson, A.; Berning, A.; Celani, P.; Cooper, D. L.; Deegan, M. J. O.; Dobbyn, A. J.; Eckert, F.; Hampel, C.; Hetzer, G.; Korona, T.; Lindh, R.; Lloyd, A. W.; McNicholas, S. J.; Manby, F. R.; Meyer, W.; Mura, M. E.; Nicklass, A.; Palmieri, P.; Pitzer, R.; Rauhut, G.; Schütz, M.; Stoll, H.; Stone, A. J.; Tarroni, R.; Thorsteinsson, T.; University College Cardiff Consultants Ltd.: Cardiff, Wales, UK, 2006.

(41) Boys, S. F.; Bernardi, F. *Mol. Phys.* **1970**, *19*, 553.

(42) Sundaralingam, M.; Jensen, L. H. *Acta Crystallogr*. **1965**, *18*, 1053.

(43) Sobolewski, A. L.; Domcke, W. *J. Phys. Chem. A* **2004**, *108*, 10917.